Quantifying the Degradation of Combined MUI and Multipath Effects in Impulse-Radio UWB

Fernando Ramírez-Mireles, *Senior Member, IEEE*

***Abstract*— We study pulse-based ultra wideband (UWB) communications over multipath channels using asynchronous spread spectrum (SS) multiple access (MA) based on time-hopping (TH) and pulse position modulated (PPM) signals. More specifically, we analyze the signal-to-interference (SIR) degradation in the presence of additive white Gaussian noise (AWGN), multi-user interference (MUI), and dense multipath effects (DME) with line-of-sight (LOS) and non-line-of-sight (NLOS). In particular, we define a *degradation margin* factor for the combined MUI and multipath effects and also find an expression for the maximum number of simultaneous radio links N_u in terms of the operating SIR, the SS processing gain, and the bit transmission rate R_b. We consider both cases with perfect and imperfect power control.**

***Index Terms*— Multipath channels, multiple access, pulse position modulation, ultra wideband communications.**

I. Introduction

Communications using UWB has been the subject of intense research activity in the last decade [1]-[5]. This work studies the performance of asynchronous pulse-based UWB PPM-TH SSMA communications under a realistic scenario that includes MUI, DME and AWGN. Several authors have studied this problem before [6]-[12]. This work differs from [10] because it considers M-ary instead of binary PPM modulation, and because it introduces the notion of degradation margin in multipath. This work differs from [11] because here we consider non-orthogonal M-ary signals instead of orthogonal M-ary signals, and because here we consider PPM-TH signals defined in terms of $M \geq 2$ time shifts with an embedded no-repetition code, using $M \geq 2$ different correlations in the receiver.

We study the performance of M-ary equally correlated (EC) PPM-TH signals with a focus on low data rate UWB systems[1], e.g., a data rate of $R_b = 100$ to 1000 kilobits per second (kbps).[2] The performance trade-off is modeled with a simple approach by finding an expression for the SIR and quantifying the degradation experienced when user one (the desired user) operates in the presence of other $N_u - 1$ users.

In single-user communications over a multipath channel the *fading margin* reflects variations in the received energy. In multiple-users communications with no multipath the *degradation factor* reflects a growth in the MUI as N_u increases. In multiple-users communications with multipath the **degradation margin**[3] reflects the combined effects of both DME and MUI. In this last case, the SIR value (dB) required to achieve a target bit error rate (BER) value BER_{spec} is

$$\begin{aligned}\overline{\text{SIR}}_{\text{rec}}(N_u) \quad \simeq \quad & \text{SIR}_{\text{spec}} + (\text{fading margin in DME}) \\ & +(\text{degradation factor with MUI}) \\ & +(\text{degradation margin with MUI in DME}),\end{aligned}$$

where SIR_{spec} is the signal-to-noise-ratio (SNR) value to achieve a desired BER_{spec} in pure AWGN.

In this work we use the BER curves to quantify this degradation margin, and then use the degradation margin to calculate an *equivalent* processing gain $\mathcal{G}_{\text{equiv}}$ (defined in Section III-B) that fits the data obtained from the BER curves. By using this approach we can relate the system parameter using simple expressions. For example,

$$\overline{N_{\text{max}}} \simeq N_{\text{max}} \, \frac{(\mathcal{G}_{\text{equiv}} \, / \, \mathcal{G})}{(\text{fading margin})},$$

where N_{max} ($\overline{N_{\text{max}}}$) and $\mathcal{G}$ ($\mathcal{G}_{\text{equiv}}$) are the maximum number of users and the processing gain, respectively, for a channel with AWGN (DME).

II. System Model

The system model and analysis follow closely [13] and [14].

A. Transmitted Signals

We consider M-ary equally correlated (EC) PPM signals [15]. The EC-PPM-TH *transmitted* signals are described by

$$\Psi^{(\nu)}_{\text{TX},j}(t) = \sum_{k=0}^{N_s-1} p_{\text{TX}}(t - kT_f - c^{(\nu)}_k T_c - a^j_k \delta), \qquad (1)$$

where t denotes time, the superscript $1 \leq \nu \leq N_u$ indicates user-dependent quantities, the index k is the number of time hops that the signal $\Psi^{(\nu)}_{\text{TX}}(t)$ has experienced, T_f is the average frame time between pulse transmissions, and $p_{\text{TX}}(t)$ is the UWB pulse used to build the transmitted PPM signals.

The a^j_k is a $0, 1$ pattern representing the j^{th} cyclic shift of an m-sequence of length N_s [16], and the index $j = 1, 2, \ldots, M$ indicates which signal from the equally-likely M-ary set is being used to transmit information. Since there are at most N_s cyclic shifts in an m-sequence we have that $2 \leq m \leq N_s$.

Manuscript received February 20, 2006; revised October 20, 2006; accepted February 9, 2007. The associate editor coordinating the review of this letter and approving it for publication was Z. Tian.

The author is with ITAM - Sistemas Digitales, Rio Hondo 1, Col. Tizapán San Angel, México City, D.F. Cp.P. 01000, México (e-mail: ramirezm@ieee.org).

Digital Object Identifier 10.1109/TWC.2007.06115.

[1]Our motivation to use PPM comes from the potential of PPM to simplify the analog front end in applications combining communications and position location.

[2]This range of R_b is in the high-end of the values $10 \leq R_b \leq 100$ kbps being considered in the standard under development by the IEEE 802.15.4a group.

[3]This degradation margin reflects the fact that MUI gets worse in the presence of DME, with more degradation as N_u increases.

The time shift value δ is chosen such that the set of signals has favorable correlation properties [15].

For a given time shift parameter T_c, the pseudo-random TH code $\{c_k^{(\nu)}\}$ provides an additional time shift to the pulse in every frame, each time shift being a discrete time value $c_k^{(\nu)}T_c$, with $0 \leq c_k^{(\nu)}T_c < N_hT_c$. The data symbol j changes only every $N_s >> 1$ hops, i.e., the system uses fast time hopping.

The UWB pulse $p_{\text{TX}}(t)$ is the basic signal used to convey information. The duration of the pulse T_p is in the order of a few nanoseconds.

B. Multiple-Path Trajectories

The link between user one's receiver and user ν's transmitter defines a multiple-path propagation trajectory that is a function of the relative position of user one's receiver with respect to the position of user ν's transmitter. This random trajectory will be identified with the random index $\xi^{(\nu)}$. There will be N_u of such trajectories, one for every pair (user ν's transmitter, user one receiver), $\nu = 1, 2, \ldots, N_u$. When user ν's transmitter radiates the signal $p_{\text{TX}}(t)$, the signal detected by user one's receiver will be represented by $p(\xi^{(\nu)}, t)$. As we move user one's receiver position with all the transmitters static, these trajectories change. Hence, the received waveforms coming from each of the transmitters also change.

C. Channel Effect in the UWB Pulse

In an ideal propagation channel, transmission of the pulse $p_{\text{TX}}(t)$ results in a received pulse $\sqrt{E_a}p(t)$ with duration T_p.[4] In an indoor multipath channel, transmission of the pulse $p_{\text{TX}}(t)$ results in a received "pulse" $\sqrt{E_a}\,p(\xi^{(\nu)}, t)$. The pulse $\sqrt{E_a}\,p(\xi^{(\nu)}, t)$ is a multipath spread version of $\sqrt{E_a}p(t)$. The average duration of $p(\xi^{(\nu)}, t)$ is denoted T_a, where T_a is a measure of the multipath delay spread, and can be up to a few hundreds of nanoseconds for indoor environments, hence $T_a >> T_p$.

The pulse $\sqrt{E_a}\ \ p(\xi^{(\nu)}, t)$ has random energy $E_p(\xi^{(\nu)}) \triangleq E_a\ \alpha^2(\xi^{(\nu)})$, where E_a is the average pulse energy, and $\alpha^2(\xi^{(\nu)}) \triangleq \int_{-\infty}^{\infty}[p(\xi^{(\nu)}, t)]^2dt$ is the normalized random energy. The pulse has normalized random signal correlation $\gamma(\xi^{(\nu)}, \delta) \triangleq \frac{\int_{-\infty}^{\infty} p(\xi^{(\nu)},t)\, p(\xi^{(\nu)},t-\delta)\, dt}{\alpha^2(\xi^{(\nu)})}$. The normalized signal cross-correlation corresponding to pulses received with two different trajectories $\xi^{(1)}$ and $\xi^{(\nu)}$ is $\tilde{\gamma}(\xi^{(1)}, \xi^{(\nu)}, \delta) \triangleq \frac{\int_{-\infty}^{\infty} p(\xi^{(1)},t)\, p(\xi^{(\nu)},t-\delta)\, dt}{\tilde{\alpha}^2(\xi^{(1)},\xi^{(\nu)})}$,where $\tilde{\alpha}^2(\xi^{(1)}, \xi^{(\nu)}) \triangleq \int_{-\infty}^{\infty} p(\xi^{(1)}, t)\, p(\xi^{(\nu)}, t)\, dt$.

D. Model for Single-User in Multipath

The PPM-TH signals received in the presence of multipath with trajectory $\xi^{(\nu)}$ are

$$\Psi_j^{(\nu)}(\xi^{(\nu)}, t) = \sum_{k=0}^{N_s-1} \sqrt{E_a}p(\xi^{(\nu)}, t - kT_f - c_k^{(\nu)}T_c - a_k^j\delta). \quad (2)$$

Since the channel is assumed to be slowly time invariant, the PPM signal is composed of shifted version of the same spreaded pulse. We will further assume that $\Psi^{(\nu)}(\xi^{(\nu)}, t)$ has fixed duration $T_s = N_sT_f$.

The signals $\Psi^{(\nu)}(\xi^{(\nu)}, t)$ have random energy $E_\Psi(\xi^{(\nu)}) = \int_{-\infty}^{\infty}[\Psi^{(\nu)}(\xi^{(\nu)}, t)]^2dt \simeq \overline{E}_s\alpha^2(\xi^{(\nu)})$, for all j, where $\overline{E}_s = N_sE_a$ is the average symbol energy. The signals have normalized random correlation values [15]

$$\begin{aligned} \beta(\xi^{(\nu)}) &\triangleq \frac{\int_{-\infty}^{\infty} \Psi_{j_1}^{(\nu)}(\xi^{(\nu)}, t)\, \Psi_{j_2}^{(\nu)}(\xi^{(\nu)}, t)\, dt}{E_\Psi(\xi^{(\nu)})} \\ &\simeq \begin{cases} 1, & j_1 = j_2, \\ \frac{1+\gamma(\xi^{(\nu)},\delta)}{2}, & j_1 \neq j_2, \end{cases} \end{aligned} \quad (3)$$

for $j_1 = 1, 2, \ldots, M$, $j_2 = 1, 2, \ldots, M$, with $N_s >> 1$. The time shift value $\delta \in (0, T_p]$ is chosen such that the *distance* between signals is maximized [15].

E. Model for the Gaussian Channel

To describe the signals in the Gaussian case we use the expressions in Sections II-C and II-D except that we suppress the random index ξ and use $\alpha^2 = 1$.

F. Model for Multiple-Users in Multipath

In the system model under consideration all the users utilize the same type of M-ary time hopping PPM signals in (1) to convey information, the difference being the TH code used for each user. All the users experience the same multipath environment, although each one has its own multipath trajectory. When N_u asynchronous transmitters are active, the received signal at user one's receiver position is

$$r(t) = \sum_{\nu=1}^{N_u} A^{(\nu)}\Psi^{(\nu)}(\xi^{(\nu)}, t - \tau^{(\nu)}) + n(t), \quad (4)$$

where $\tau^{(\nu)}$ represent time asynchronisms between the clock of user ν's transmitter and user one's receiver, $(A^{(\nu)})^2$ is the ratio of average power used by user ν's transmitter with respect to the average power used by user one's transmitter (with $|A^{(1)}|^2 = 1$), and $n(t)$ represents non-MA interference modeled as AWGN with two-sided power spectrum density (PSD) $N_o/2$.

G. Statistical Averages

The signal $r(t)$ in (4) is a random process that depends on the random noise $n(t)$ and three other types of random variables: The random time delays, the random time hopping codes, and the random multiple-path trajectories indexes. Performance computation is based on SIR ratios and bit error rates (BER) rates averaged over all random variables. The receiver will be assumed to be perfectly synchronized.

To facilitate our analytical treatment, we make assumptions similar to [13] [14]. For the low data rates under consideration the effect of the MUI at the output of the correlation receiver can be modeled as a zero mean Gaussian random variable with *random (position-dependent)* variance.[5]

[4]Under free space propagation conditions the received pulse $p(t)$ has been modeled as the derivative of the transmitted pulse $p_{\text{TX}}(t)$. This model for the antenna system has been repeatedly used [1]-[5]. Most existing UWB antennas do not have that frequency response. Even for those antennas systems, the results in this work still can be applied since the analysis is based on the energy and correlation values of the *received* signals.

[5]For discussions on the validity of the Gaussian assumption for low values of N_s and N_u see [17]-[21].

III. Receiver Signal Processing and Performance

We will present results for EC-PPM signals. The analysis can be generalized to signal sets with other correlation properties.

To simplify notation, in the following analysis we will drop the super-index (1) from $\Psi^{(1)}(\xi^{(1)},t)$, $A^{(1)}$, $\tau^{(1)}$, and $c^{(1)}$.

A. Signal Detection and BER

Let's assume that the receiver wants to demodulate user one's signal. The received signal $r(t)$ in (4) can be rewritten

$$r(t) \;=\; A\Psi(\xi, t-\tau) + n_{\text{TOT}}(t),\; t \in \mathcal{T},$$

where $\mathcal{T} \triangleq [\tau, N_s T_f + \tau]$, and

$$n_{\text{TOT}}(t) \triangleq \sum_{\nu=2}^{N_u} A^{(\nu)}\Psi^{(\nu)}(\xi^{(\nu)}, t-\tau^{(\nu)}) + n(t).$$

For the time being, let's assume that user one's receiver is static at one place, and that user one's transmitter is at a fixed position, i.e., ξ is kept fixed.

In the present analysis signal detection is achieved using a Rake receiver [22]. The performance of such correlation receiver can be analyzed using traditional detection theory [23], and the demodulation problem can be analyzed as the time-shift-coherent detection of M equal-energy, equally-likely signals in the presence of Gaussian interference plus noise using a M-ary correlation receiver. The resulting performance results should be considered as a lower bound, i.e., performance of an ideal Rake receiver.

To estimate the BER for time-shift-coherent detection of equi-correlated signals we will use the union bound

$$\text{UBPe}(N_u|\xi) = \frac{M}{2}\int_{\sqrt{\log_2(M)\,\text{SIR}(N_u|\xi)}}^{\infty} \frac{\exp(-\rho^2/2)}{\sqrt{2\pi}}\, d\rho. \tag{5}$$

where

$$\text{SIR}_{\text{out}}(N_u|\xi) \;\triangleq\; \frac{1}{[\text{SIR}(1|\xi)]^{-1}+[\text{SIR}_{\text{MUI}}(N_u|\xi)]^{-1}}, \tag{6}$$

is the output bit SIR observed in the presence of N_u-1 other users,

$$\text{SIR}(1|\xi) \;\triangleq\; \frac{\overline{E}_b\,\alpha^2(\xi)\,[1-\beta(\xi)]}{N_o}, \tag{7}$$

is the SNR when only user one is active,

$$\text{SIR}_{\text{MUI}}(N_u|\xi) \;\triangleq\; \frac{\overline{E}_b\alpha^2(\xi)[1-\beta(\xi)]}{N_{\text{MUI}}(\xi)} \simeq \frac{\mathcal{G}(\xi)}{(N_u-1)}, \tag{8}$$

is the SIR in the presence of MUI and in the absence of AWGN, $\overline{E}_b = \frac{\overline{E}_\Psi}{\log_2(M)}$ is the average bit energy, and where

$$N_{\text{MUI}}(\xi) \;\triangleq\; \frac{(N_u-1)\,\overline{E}_b\alpha^2(\xi)}{\mathcal{G}(\xi)}[1-\beta(\xi)], \tag{9}$$

is the *equivalent* PSD level of the total MUI under ideal power control conditions, where

$$\begin{aligned}
\mathcal{G}(\xi) &\triangleq \frac{(\mu(\xi)/T_f)}{R_b},\\
\mu(\xi) &= \frac{m_p^2(\xi,\xi,0,0,\delta)}{2\,\sigma_p^2(\xi,0,\delta)},\\
\sigma_p^2(\xi,\theta,\eta) &\triangleq \mathbf{E}_{(\xi^{(\nu)}|\xi)}\{\sigma_p^2(\xi,\xi^{(\nu)},\theta,\eta)\},\\
\sigma_p^2(\xi,\xi^{(\nu)},\theta,\eta) &\triangleq T_f^{-1}\int_{-T_f/2}^{T_f/2} m_p^2(\xi,\xi^{(\nu)},\varsigma,\theta,\eta)\,d\varsigma,
\end{aligned}$$

where R_b is the bit transmission rate, and where

$$\begin{aligned}
&m_p(\xi,\xi^{(\nu)},\varsigma,\theta,\eta)\\
&\triangleq \int_{-\infty}^{\infty} p(\xi^{(\nu)},\varrho-\varsigma)\;[p(\xi,\varrho-\theta)-p(\xi,\varrho-\eta)]\,d\varrho\\
&= \begin{cases}
\alpha^2(\xi)\times \\
[\gamma(\xi,\varsigma-\theta)-\gamma(\xi,\varsigma-\eta)], & \text{for } \nu=1,\\
\tilde{\alpha}^2(\xi,\xi^{(\nu)})\times \\
\left[\tilde{\gamma}(\xi,\xi^{(\nu)},\varsigma-\theta)-\tilde{\gamma}(\xi,\xi^{(\nu)},\varsigma-\eta)\right], & \text{for } \nu\neq 1,
\end{cases}
\end{aligned}$$

The $\mathcal{G}(\xi)$ is a *random* processing gain factor, and $\mu(\xi)$ is a normalized SIR parameter defined in terms of both the received UWB pulse shape and the time-shift defining the PPM data modulation.[6] The averaged performance can be obtained by taking the expected value $\mathbf{E}_\xi\{\cdot\}$ of (5) over all values of ξ to get

$$\overline{\text{UBPe}}\left(\frac{\overline{E}_b}{N_o}, N_u\right) \;\triangleq\; \mathbf{E}_\xi\{\text{UBPe}\,(N_u|\xi)\}. \tag{10}$$

B. Multiple Access Performance

Notice that $\overline{\text{SIR}}(1) \triangleq \mathbf{E}_\xi\{\text{SIR}(1|\xi)\}$ is the average SNR value in the presence of AWGN and DME, and that $\overline{\text{SIR}}_{\text{out}}(N_u) \triangleq \mathbf{E}_\xi\{\text{SIR}_{\text{out}}(N_u|\xi)\}$ is the average SIR value in the presence of AWGN, DME and MUI. Naturally, $\overline{\text{SIR}}_{\text{out}}(N_u) < \overline{\text{SIR}}(1)$

Let $\overline{\text{SIR}}_{\text{spec}}$ be the specified operating SIR to achieve a desired BER_{spec} in a single users system. Let $\overline{\text{SIR}}_{\text{rec}}(N_u) > \overline{\text{SIR}}_{\text{spec}}$ be the required value of $\overline{\text{SIR}}(1)$ that makes $\overline{\text{SIR}}_{\text{out}}(N_u) = \overline{\text{SIR}}_{\text{spec}}$ so BER_{spec} can be achieved in the presence of MUI.

Using the relations in (6),(7),(8), we now define the degradation factor in multipath

$$\begin{aligned}
\text{DF}_{\text{MP}}(N_u) &\triangleq \frac{\overline{\text{SIR}}_{\text{rec}}(N_u)}{\overline{\text{SIR}}_{\text{spec}}} = \frac{(\frac{\overline{E_b}}{N_o})_{\text{rec}}}{(\frac{\overline{E_b}}{N_o})_{\text{spec}}}\\
&= \frac{1}{1-(\frac{\overline{E_b}}{N_o})_{\text{spec}}\left[\frac{(N_u-1)}{\mathcal{G}_{\text{equiv}}}\right]} \;\geq\; 1.
\end{aligned} \tag{11}$$

This definition requires to know the value of the *equivalent* processing gain $\mathcal{G}_{\text{equiv}}$. Notice that $\mathcal{G}_{\text{equiv}}$ satisfy the relation

$$\overline{\text{UBPe}}\left((\frac{\overline{E_b}}{N_o})_{\text{spec}} \times \text{DF}_{\text{MP}}(N_u),\; N_u\right) \simeq \text{BER}_{\text{spec}}, \tag{12}$$

[6]Notice that we can re-write $\mathcal{G}(\xi) = K_\mu(\xi)\frac{T_f}{T_p}N_s$, where $K_\mu(\xi)$ is a time-normalized version of $\mu(\xi)$.

i.e., the SNR value $(\frac{E_b}{N_o})_{\text{spec}} \times \text{DF}_{\text{MP}}(N_u)$ becomes a function of $\mathcal{G}_{\text{equiv}}$, and the desired value of $\mathcal{G}_{\text{equiv}}$ is the one that makes the relation (12) to hold.

From (11) we can find

$$N_u(\text{DF}_{\text{MP}}) = \lfloor \frac{\mathcal{G}_{\text{equiv}}}{(\frac{E_b}{N_o})_{\text{spec}}}(1 - \frac{1}{\text{DF}_{\text{MP}}}) \rfloor + 1, \quad (13)$$

where $\lfloor \cdot \rfloor$ is the floor operation.

For comparison purposes, we also define a MUI-DME *degradation margin*

$$\Delta\text{DF}(N_u) \stackrel{\triangle}{=} \text{DF}_{\text{MP}}(N_u) - \text{DF}_{\text{AWGN}}(N_u), \quad \text{(in dB)} \quad (14)$$

where $\text{DF}_{\text{AWGN}}(N_u) \stackrel{\triangle}{=} \frac{\text{SIR}_{\text{rec}}(N_u)}{\text{SIR}_{\text{spec}}}$ is the degradation factor in AWGN.[7]

IV. Numerical Results

A. UWB Pulses and Parameters

The UWB pulse considered in this example are based on pulsed sine waves with center frequency 5 GHz and parameters $T_p = 2$ ns and $T_a = 160$ ns as described in [25] using the channel model in [26] [27]. We also use $\delta = 0.1$ ns, $T_f = 200$ ns and $R_b = 200$ Kbps per user. With these values we get $N_s = \frac{\log_2(M)}{R_b\, T_f} \simeq 25\log_2(M)$, a value large enough to reasonably justify the Gaussian assumption for the MUI for low values of N_u. Finally, we set the target $\text{BER}_{\text{spec}} \simeq 10^{-6}$.

B. Averages in AWGN and Multipath

Calculation in the Gaussian channel use the expressions in Section III with $\alpha^2 = 1$, $\beta = 0.025$, suppressing both the random index ξ and the bar $\overline{(\cdot)}$, and using $\mathcal{G}$ instead of $\mathcal{G}_{\text{equiv}}$.

Calculations in multipath require averaging over ξ as in [14], but using the sample mean values

$$\overline{\text{UBPe}}\left(\tfrac{E_b}{N_o}, N_u\right) \approx \tfrac{1}{Q}\textstyle\sum_{\xi=1}^{Q} \text{UBPe}\,(N_u|\xi)\,,$$

$$\mu(\xi) \approx \frac{m_p^2(\xi,\xi,0,0,\delta)}{2\,\sigma_p^2(\xi,0,\delta)},$$

$$\sigma_p^2(\xi,0,\delta) \approx \tfrac{1}{(Q-1)}\textstyle\sum_{\substack{i=1\\ \xi_i\neq\xi}}^{Q} \sigma_p^2(\xi,\xi_i,0,\delta)$$

$$\sigma_p^2(\xi,\xi_i,0,\delta) \approx T_f^{-1}\int_{-T_f/2}^{T_f/2} m_p^2(\xi,\xi_i,\varsigma,0,\delta)\,d\varsigma,$$

where $Q = 200$ is the size of the sample for every transmitter-receiver separation distance D. Results were averaged considering $D = 3, 6, 9$ meters for the LOS case and $D = 1, 2, 3$ meters for the NLOS case.

C. Calculations With Perfect (Average) Power Control

We first determine the BER curves for $2 \leq M \leq 64$ and $N_u = 1$ (Fig. 1(a)), and from these curves we determine $(\frac{E_b}{N_o})_{\text{spec}}$ for different M corresponding to $\text{BER}_{\text{spec}} \simeq 10^{-6}$ (see Table I). Next we calculate μ, $\mathcal{G}$, $\mu(\xi)$ and $\mathcal{G}(\xi)$, and proceed to determine the BER curves for $M = 2$ and $N_u > 1$ (Fig. 1(b)) and for $M = 64$ and $N_u > 1$ (Fig. not shown).

[7]The degradation factor in AWGN was defined in [24]. Degradation factor in DME was used in [10]. In this work we are expressing the degradation factor in terms of the *equivalent* processing gain.

TABLE I

Values of SIR, fading margin, and processing gain for different M for $R_b = 200$ kbps with $\text{BER}_{\text{spec}} \simeq 10^{-6}$.

M	$(\frac{E_b}{N_o})_{\text{spec}}$ AWGN (dB)	$(\frac{E_b}{N_o})_{\text{spec}}$ LOS (dB)	$(\frac{E_b}{N_o})_{\text{spec}}$ NLOS (dB)	$\mathcal{G}$ AWGN	$\mathcal{G}_{\text{equiv}}$ LOS	$\mathcal{G}_{\text{equiv}}$ NLOS
2	13.53	22.20	25.58	3569	3500	3520
4	10.80	19.65	23.05	3569	3500	3520
8	9.25	18.29	21.67	3569	3500	3520
16	8.23	17.43	20.80	3569	3500	3520
32	7.46	16.80	20.17	3569	3500	3520
64	6.90	16.33	19.65	3569	3500	3520

TABLE II

Approximate (maximum) values of N_u to achieve $\text{BER}_{\text{spec}} \simeq 10^{-5}$ for different R_b using $M = 2$. Left columns: Perfect average power control (pure AWGN, LOS, and NLOS). Right columns: Imperfect power control in AWGN (LOS and NLOS energy statistics).

R_b (Kbps)	N_u (AWGN)	N_u (LOS)	N_u (NLOS)	N_u (AWGN-LOS)	N_u (AWGN-NLOS)
100	76	24	11	30	14
200	37	12	6	15	7
300	25	8	4	11	5
400	19	6	3	8	4
500	15	5	2	7	3
600	12	4	2	6	3
700	10	3	2	5	3
800	9	3	2	4	2
900	8	3	2	4	2
1000	8	3	2	4	2

From the BER curves for $N_u > 1$ we determine the *true* value of $\text{DF}_{\text{MP}}(N_u)$. From this *true* value $\text{DF}_{\text{MP}}(N_u)$ and knowing $(\frac{E_b}{N_o})_{\text{spec}}$ we determine $\mathcal{G}_{\text{equiv}}$ (see Table I) such that $\mathcal{G}_{\text{equiv}}$ and $(\frac{E_b}{N_o})_{\text{spec}}$ in (11) produce an *equivalent* version of $\text{DF}_{\text{MP}}(N_u)$ that fits the true value of the degradation factor[8] (both *true* and *equivalent* versions of $\text{DF}_{\text{MP}}(N_u)$ are plotted in Fig. 1(c) and there is a good fit).[9] Next, we use this $\mathcal{G}_{\text{equiv}}$ and the other parameters to determine N_u in (13) for $2 \leq M \leq 64$ with fixed $R_b = 200$ Kbps as depicted in Fig. 1(d). Finally, we can also use this $\mathcal{G}_{\text{equiv}}$ and the other parameters in Table I to determine $\Delta\text{DF}(N_u)$ in (14) (results not shown).

Furthermore, the first four columns in Table II shows the maximum values of N_u to achieve a value of $\text{BER}_{\text{spec}} \simeq 10^{-5}$ for different R_b using $M = 2$. Notice that in this case a different processing gain is calculated for every value of R_b.

D. Calculations in AWGN With Imperfect Power Control

To study the performance in the presence of AWGN and MUI with no DME but with imperfect power control, we make calculation with $\alpha^2 = 1$, $\beta = 0.025$, and we use $(\frac{E_b}{N_o})_{\text{spec}} = 13.58$ dB (i.e., zero fading margin) but we let $\mathcal{G}(\xi)$ vary randomly in (9), with the random power variations of the components of the MUI following the statistics of α^2 in both

[8]Notice that in the Gaussian case both the *true* and the *equivalent* $\text{DF}(N_u)$ are the same.

[9]Notice that the *true* $\text{DF}_{\text{MP}}(N_u)$ is found from the BER curves already averaged over the multipath effects, while the *equivalent* $\text{DF}_{\text{MP}}(N_u)$ is not a direct average of different realizations of a random degradation factor, but comes from a model in (11) that fits the BER curves.

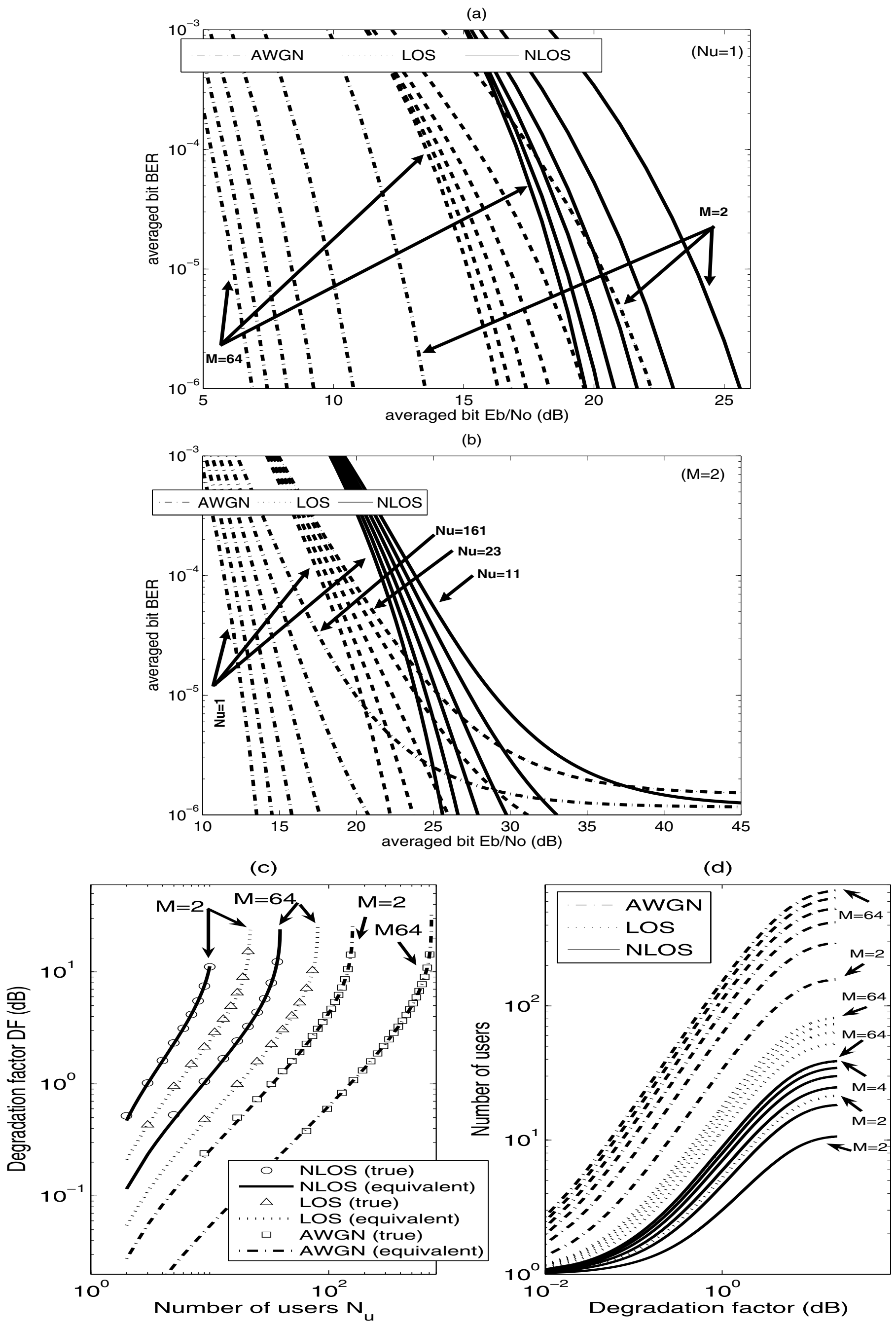

Fig. 1. (a) The $\overline{\text{UBPe}}\left(\frac{\overline{E}_b}{N_o}, N_u\right)$ for $2 \leq M \leq 64$ with $N_u = 1$, (b) the $\overline{\text{UBPe}}\left(\frac{\overline{E}_b}{N_o}, N_u\right)$ for $M = 2$ with $N_u = 1, 33, 65, 97, 129, 161$ (AWGN), $N_u = 1, 7, 13, 19, 23$ (LOS), and $N_u = 1, 3, 5, 7, 9, 11$ (NLOS), (c) *True* and *equivalent* versions of $\text{DF}_{\text{AWGN}}(N_u)$ and $\text{DF}_{\text{MP}}(N_u)$ for $M = 2$ and 64, (d) the $N_u(\text{DF}_{\text{MP}})$ for $2 \leq M \leq 64$, calculated using the *equivalent* values of the degradation factor. Results are for $R_b = 200$ kbps with $\text{BER}_{\textbf{spec}} \simeq 10^{-6}$.

LOS and NLOS cases. The last two columns in table II shows N_u to achieve $\text{BER}_{\textbf{spec}} \simeq 10^{-5}$ for different R_b with $M = 2$:

V. Conclusions

This work studies the performance of pulse-based UWB SSMA communications in the presence of AWGN, MUI, and DME. More specifically, we quantify the degradation of combined MUI and multipath effects in Impulse-Radio UWB. We proposed a model of the degradation that allows us to calculate the number of users in the system. The model is found for $M = 2$ and $M = 64$ and then used for $2 \leq M \leq 64$. In general, the results show that:

- As N_u increases, $\text{DF}_{\text{MP}}(N_u)$ also increases, and $\overline{\text{SIR}}_{\textbf{rec}}(N_u)$ must be increased in order to maintain the $\text{BER}_{\textbf{spec}}$. Ultimately, however, no amount of increase in $\overline{\text{SIR}}_{\textbf{rec}}(N_u)$ can offset the effects of the MUI, and N_u reaches a plateau with a maximum number of users equal to the ratio $\mathcal{G}_{\textbf{equiv}}/(\overline{E}_b/N_o)_{\textbf{spec}}$ (see Fig. 1(d)).
- We can relate the maximum number of users $\overline{N_{\text{max}}} \simeq N_{\text{max}}\ (\frac{\mathcal{G}_{\textbf{equiv}}}{\mathcal{G}})$ / (fading margin). From table I we notice that there is little difference in $\mathcal{G}_{\textbf{equiv}}$ for LOS and NLOS. Hence, the main difference in performance come from the difference in fading margin (see Figs. 1(b) and 1(d)).

- M-ary modulation can be used to compensate for degradation caused by the combined effects of both MUI and DME,[10] and we can relate $N_{\max}^{(M)} \simeq C_M \, N_{\max}^{(2)}$, for $M \geq 2$, where the $C_M = \mathrm{SIR}_{\mathbf{spec}}^{(2)}/\mathrm{SIR}_{\mathbf{spec}}^{(M)}$ is the coding gain for $M \geq 2$. In particular, even that $N_{\max}^{(64)}/N_{\max}^{(2)} \simeq C_{(64)}$, we found that

$$\mathrm{DF}^{(64)}/\mathrm{DF}^{(2)} \simeq \frac{1}{C_{(64)}} \frac{N_{\max}^{(64)} - C_{(64)}[N_u - 1]}{N_{\max}^{(2)} - \frac{1}{C_{(64)}}[N_u - 1]}.$$

- For the particular system model that we use, we found that imperfect power control degrade the number of users in the same order of reduction produced by MUI combined with DME. In DME with perfect average power control, both the signal and the interference suffer fading. In AWGN with imperfect power control, the energy of the signal is constant (no fading) and the energy of the MUI follows the statistics of a multipath channel. On average, the first situation (combined effects of fading and multiuser interference) is worse than the later (no fading margin for the signal of interest).

VI. Acknowledgments

The author thanks the anonymous reviewers for their comments that helped to improve the quality of the paper. He also thanks Dr. Robert A. Scholtz for his guidance and encouragement during the author's Ph.D. program and after that.

References

[1] *Special Issue on Ultra-Wideband Radio in Multiaccess Wireless Communications, IEEE J. Select. Areas Commun.*, vol. 20, no. 9, Dec. 2002.
[2] *Special Issue on UWB - State of the Art, EURASIP J.*, vol. 2005, no. 3, Mar. 2005.
[3] *Special Issue on UWB Wireless Communications - A New Horizon, IEEE Trans. Veh. Technol.*, vol. 54, no. 5, Sep. 2005.
[4] *Special Issue: Ultra Wideband for Wireless Communications, Wireless Commun. Mobile Comput.*, vol. 5, no. 5, Aug. 2005.
[5] *Special Issue on Ultra-Wideband Communications, IEEE J. Select. Areas Commun.*, vol. 24, no. 4, pt. 1, Apr. 2006.
[6] C. J. Le Martret and G. B. Giannakis, "All-digital impulse radio with multiuser detection for wireless cellular systems," *IEEE Trans. Commun.*, vol. 50, no. 9, pp. 1440-1450, Sep. 2002.
[7] Q. Li and L. A. Rusch, "Multiuser receivers for DS-CDMA UWB," in *Proc. IEEE UWBST Conf.*, May 2002, pp. 163-167.
[8] J. R. Foester, "The performance of a direct-sequence spread ultra-wideband system in the presence of multipath, narrowband interference and multiuser interference," in *Proc. IEEE UWBST Conf.*, May 2002, pp. 87-91.
[9] L Yang and G. B. Giannakis, "Impulse radio multiple access through ISI channels with multi-stage block-spreading," in *Proc. IEEE UWBST Conf.*, May 2002, pp. 277-281.
[10] A. Taha and K. M. Chugg, "Multipath diversity reception of wireless multiple access time-hopping digital impulse radio," in *Proc. IEEE UWBST Conf.*, May 2002, pp. 283-288.
[11] G. Durisi, et al., "A general method for error probability computation of UWB systems for indoor multiuser communications," *J. Commun. Networks*, vol. 5, no. 4, pp. 354-364, Dec. 2003.
[12] C. J. Le Martret, A-L Deleuze, and P. Ciblat, "Optimal time-hopping codes for multi-user interference mitigation in ultra-wide bandwidth impulse radio," *IEEE Trans. Wireless Commun.*, vol. 5, no. 6, pp. 1516-1525, June 2006.
[13] F. Ramírez-Mireles, "Performance of ultrawideband SSMA using time hopping and M-ary PPM," *IEEE J. Select. Areas Commun.*, vol. 19, pp. 1186-1196, June 2001.

[10]The effect of jitter in M ary PPM-TH signals in the presence of MUI is studied in [28].

[14] ——, "On performance of ultra wideband signals in Gaussian noise and dense multipath," *IEEE Trans. Veh. Technol.*, vol. 50, pp. 244-249, Jan. 2001.
[15] F. Ramírez-Mireles and R. A. Scholtz, "Time-shift-keyed equicorrelated signal sets for impulse radio M-ary modulation," in *Proc. IEEE Wireless Conf.*, July 1998, pp. 404-408.
[16] S. W. Golomb, "Construction of signals with favorable correlation properties," *Surveys in Combinatorics*, London Mathematical Society Lecture Notes Series 166, Cambridge University Press, 1991.
[17] G. Durisi and G. Romano, "On the validity of Gaussian approximation to characterize the multiuser capacity of UWB TH PPM," in *Proc. IEEE UWBST Conf.*, May 2002, pp. 157-161.
[18] J. Fiorina and W. Hachem, "On the asymptotic distribution of the correlation receiver output for time-hopped UWB signals," *IEEE Trans. Signal Processing,* vol. 54, pp. 2529-2545, July 2006.
[19] Y. Dhibi and T. Kaiser, "On the impulsiveness of multiuser interferences in TH-PPM-UWB systems," *IEEE Trans. Signal Processing,* vol. 54, pp. 2853-2857, July 2006.
[20] G. Giancola, L. De Nardis, and M.-G. Di Benedetto, "Multi user interference in power-unbalanced ultra wide band systems: Analysis and verification," in *Proc. IEEE UWBST Conf.*, Nov. 2003, pp. 325-329.
[21] F. Ramírez-Mireles and A. Almada, "Testing the Gaussianity of UWB TH-PPM MUI with imperfect power control and multipath," submitted to *IEEE MILCOM 2007 Conf.*
[22] J. G. Proakis, *Digital Communications*. New York: McGraw-Hill, 1995, pp. 797-805.
[23] R. M. Gagliardi, *Introduction to Communications Engineering*, 2nd ed. Hoboken, NJ: John Wiley and Sons, 1988.
[24] C. L. Weber, G. K. Huth, and B. H. Batson, "Performance considerations of code division multiple-access systems," *IEEE Trans. Veh. Technol.*, vol. 30, no. 1, pp. 3-9, Feb. 1981.
[25] R. Bastidas-Puga, F. Ramírez-Mireles, and D. Muñoz-Rodríguez, "On fading margin in ultrawideband communications over multipath channels," *IEEE Trans. Broadcasting*, vol. 51, no. 3, pp. 366-370, Sep. 2005.
[26] W. Turin, R. Jana, S. Ghassemzadeh, C. Rice, and V. Tarokh, "Autoregressive modeling of an indoor UWB channel," in *Proc. IEEE UWBST Conf.*, May 2002, pp. 71-74.
[27] S. Ghassemzadeh, R. Jana, C. Rice, W. Turin, and V. Tarokh, "A statistical path loss model for in-home UWB channel," in *Proc. IEEE UWBST Conf.*, May 2002, pp. 59-64.
[28] N. V. Kokkalis, P. T. Mathiopoulos, G. K. Karagiannidis, and C. S. Koukourlis, "Performance analysis of M-ary PPM TH-UWB systems in the presence of MUI and timing jitter," *IEEE J. Select. Areas Commun.*, vol. 24, no. 4, pp. 822-828, Apr. 2006.